RSC Advances

ROYAL SOCIETY OF CHEMISTRY

www.rsc.org/advances

RSC Advances

RSCPublishing

ARTICLE

Improved electrode durability using a boron-doped diamond catalyst support for proton exchange membrane fuel cells

Cite this: DOI: 10.1039/x0xx00000x

Jungdo Kim, Yoon-Soo Chun, Seung-Koo Lee, and Dae-Soon Lim*

Table of contents

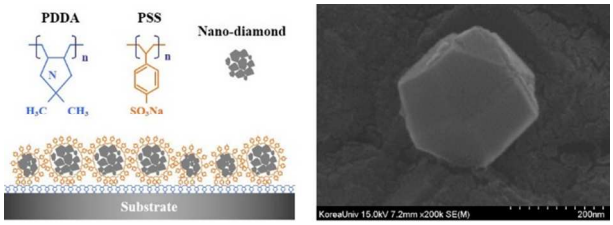

BDD was produced by an electrostatic self-assembly (ESA) method. We investigated the improvement of durability by performing under real PEMFC operating conditions and observing changes in the support material morphology.

Received 00th October 2014,
Accepted 00th xxxxx xxxx

DOI: 10.1039/x0xx00000x

www.rsc.org/advances

Abstract

The durability of a fuel cell electrode was improved by using a boron-doped diamond (BDD) electrode support. BDD nanoparticles was synthesized by a size-controllable electrostatic self-assembly method (ESA). Moreover, the morphological changes as a function of operating time were investigated to prove the durability enhancement. First, diamond seeds were formed by an ESA method. The BDDs were then synthesized around these seeds by a conventional hot-filament chemical vapor deposition process. A Pt catalyst was then deposited by the polyol method, and it was characterized by scanning electron microscopy and transmission electron microscopy. The supporting BDD particles were 100–200 nm in size, whereas the Pt catalyst particles were 2–4 nm. Multiwalled carbon nanotubes (MWCNTs) and a conventional supporting material (Vulcan XC-72) were also studied for comparison. The electrochemical characteristics were examined by cyclic voltammetry and unit cell tests. The BDD support showed a larger surface area and better performance than the MWCNT and Vulcan XC-72 supports. According to the accelerated long-term stability tests, the BDD support material was more stable than the MWCNT and Vulcan XC-72 supports. These results show that BDD supports improve the durability of the fuel cell electrode.

Introduction

Numerous researchers have investigated proton exchange membrane fuel cells (PEMFCs) owing to their high energy efficiency, relatively low operating temperature, and rapid operation.[1-4] However, the commercial application of PEMFCs remains hindered by several problems. As a result of their low corrosion resistance during operation, a considerable amount of platinum, expensive electrolyte membranes, bipolar plates, etc. are required, which drives the development of alternative materials and improved performance.[5,6] Moreover, this durability limitation is a primary problem in commercializing PEMFCs,[7-10] and it has recently been recognized as a vital issue that needs to be addressed before commercialization of PEMFCs can proceed. For this reason, improving the durability of every part of PEMFCs has been widely researched, including the use of composite materials for the bipolar plate,[11-13] platinum catalyst alloys,[14-18] and non-noble metal materials, and improved durability has been reported.[19-21] However, problems still remain owing to the acidic operating environment of PEMFCs, and thus further research on improving durability is needed.

The dissolution of Pt-based catalysts and corrosion of the catalyst support are the main causes of catalyst degradation under PEMFC operation. To protect against catalyst dissolution and catalyst support corrosion, the use of water-fluxing,[22] pre-leaching,[23] and additives[24] have been investigated. Also, research on alternative catalyst support materials has recently been reported.[25,26] Among these catalyst support materials, carbon is the most frequently used material under normal conditions. However, carbon is destroyed under the PEMFC operating conditions, which include high temperatures, high potentials, high water content, and low pH. This corrosion of carbon weakens the attachment of catalyst particles to the support surface, decreasing its conductivity and performance. For this reason, some have reported that boron-doped diamond (BDD) can be used as a support material. Avaca *et al*.[27] prepared a BDD support material by grinding a BDD film, and they produced platinized catalysts by the sol–gel method. Swain *et al*.[28] reported the production of an electrocatalyst support by overcoating the high surface area of diamond powder with a thin layer of BDD. Reported results demonstrated that platinized diamond was more resistant to oxidation than platinized Vulcan XC-72. However, understanding the durability and degradation mechanisms of platinized diamond under real cell conditions is limited.

In this study, BDD was produced by an electrostatic self-assembly (ESA) method. With the ESA method, the size of the support can be controlled to less than 200 nm and well-separated particles can be obtained by controlling the processing time. We investigated the improvement of durability by performing under real PEMFC operating conditions and observing changes in the support material morphology. The performance of the BDD support material was compared with those of Vulcan XC-72, which is the most frequently used material for catalyst supports, and multi-walled carbon nanotubes by observing morphology changes as a function of time. The enhanced durability and performance resulting from the application of the BDD support were confirmed by unit cell tests and long-term stability tests.

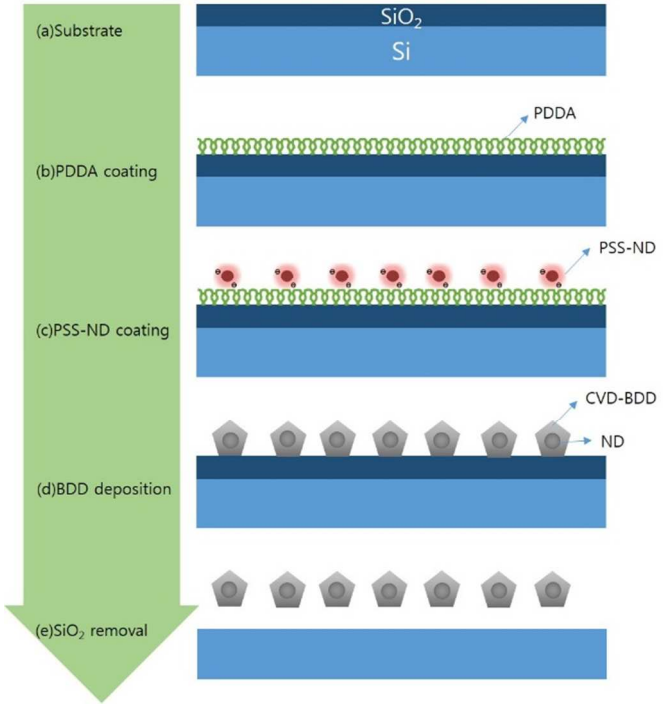

Experimental

Production of support material

Fig. 1 shows the preparation procedure for the BDD support using the ESA method. First, attrition-milled nanodiamond (ND) particles were seeded onto pretreated SiO_2-coated silicon substrates by the ESA method.[29] During the attrition-milling process, the anionic polyelectrolyte [poly(sodium 4-styrenesulfonate), PSS] was added to produce a negatively charged coating on the nanodiamond surface (PSS-ND). The substrate was then dipped into a cationic aqueous solution [poly(diallyldimethylammonium chloride) PDDA, M_w: 400,000–500,000] for 1 day, followed by a 1 min dip in the anionic PSS-ND aqueous solution. After the ESA process, the BDD support materials were synthesized on the nanodiamond-seeded silicon substrates by conventional hot-filament chemical vapor deposition (HF-CVD). During the BDD support synthesis, the substrate temperature was kept at 470 °C and the deposition time was 4 h. To separate the BDD support materials from the underlying silicon substrate, hydrofluoric acid was used to etch the SiO_2 layer. The BDD support materials obtained by this method were confirmed by X-ray diffraction (XRD, model D/MAX-2500V/PC, Rigaku), transmission electron microscopy (TEM), and selected area electron diffraction (SAED) pattern analyses.

Fig. 1. Schematic of the steps used to produce the BDD support: (a) the substrate used for BDD growth, (b) initial coating of the PDDA, (c) deposition of the PSS-wrapped NDs, (d) deposition of the BDD through CVD around the NDs, and (e) removal of the SiO_2 to separate the BDDs

Production of the electrocatalyst

Three different electrocatalysts were prepared by a modified polyol method,[30] where ethylene glycol was used as a reducing agent and a solvent. The ESA/HF-CVD-produced BDD, a commercial carbon powder (Vulcan XC-72), and MWCNTs were used to compare electrocatalyst support performance. A Pt precursor, chloroplatinic acid hexahydrate ($H_2PtCl_6 \cdot 6H_2O$, Aldrich), was prepared as a 0.01 M stock solution to prevent Pt salt hydration. The Pt salt stock solution was mixed individually with each support material and stirred for 30 min. The mixed solutions were placed into a dropper and dropped at a rate of 2 mL/min into the reducing agent heated to a 180–190 °C temperature in a reactor. The reactor was maintained at the reaction temperature for 30 min and then cooled to room temperature in air. The Pt electrocatalysts were obtained after the resultant suspension was washed with deionized water, filtered through a nylon membrane, and dried for several hours. In this study, 20 wt% Pt/support electrocatalysts were produced and their morphology and distribution were identified by TEM.

Electrochemical measurements

Membrane electrode assemblies (MEAs) with a 5 cm^2 active area were fabricated by hot pressing. The prepared Pt/BDD, Pt/Vulcan XC-72, and Pt/MWCNT electrocatalysts were used as the respective cathodes. A commercial E-TEK electrode loaded with 0.4 mg/cm^2 of Pt was used as the anode. The anode and the cathode were arranged in a sandwich form with a layer of Nafion® 212 [pretreated with hydrogen peroxide (H_2O_2) and sulfuric acid (H_2SO_4) solutions] between them. The resulting MEAs were pressed at 170 $kg \cdot f \cdot cm^{-2}$ (17 MPa) and a temperature of 140 °C for 90 s.

The unit cell test was carried out at 80 °C under atmospheric pressure using hydrogen gas (H_2) as the fuel and oxygen gas (O_2) as the oxidant. The fuel and oxidant were injected into the cell through separate humidifiers at 80 and 75 °C, respectively, at a flow rate of 150 $mL \cdot min^{-1}$. The cell performance was evaluated with an electronic loader (ESL-300Z, CNL).

The electrochemical measurements were performed at 80 °C on a 5 cm^2 electrode area unit cell across a potential range of 50 mV to 1.2 V *vs*. a reversible hydrogen electrode (RHE) with a 50 $mV \cdot s^{-1}$ sweep rate. In these measurements, the anode was used as the reference and counter electrode and the cathode was used as the working electrode.

Accelerated long-term stability tests

Accelerated long-term stability tests for 100 h of cell operation were performed. Each catalyst, *i.e.*, Pt/ Vulcan XC-72, Pt/MWCNT, and Pt/BDD, was coated onto an individual electrode. During the accelerated stability tests, the voltage was maintained at 0.6 V and the unit cells were kept at 90 °C, which was a higher temperature than that of normal PEMFC operation (70–80°C). The tests were carried out for a total of 100 h, with scanning electron microscopy (SEM) images taken at 30 h, 60 h, and 100 h in order to check the morphology.

Results and disccusions

Characterization of the electrocatalyst

The phases of the prepared electrocatalysts were identified using XRD. Fig. 2 shows the XRD pattern of the Pt/BDD electrocatalyst prepared by the ESA/polyol method. Three Pt peaks at 2θ of ~40°, ~47°, and ~68° can be seen, which correspond to Pt (1 1 1), Pt (2 0 0), and Pt (2 2 0), respectively. The average size of the electrocatalyst particles is estimated to be 2.5 nm from the (2 2 0) peak using the Scherrer formula. There is a narrow peak at 2θ of ~44°, which indicates the diamond (1 1 1) phase, as verified with JCPDS. Therefore, the XRD results confirm the formation of diamond phases.

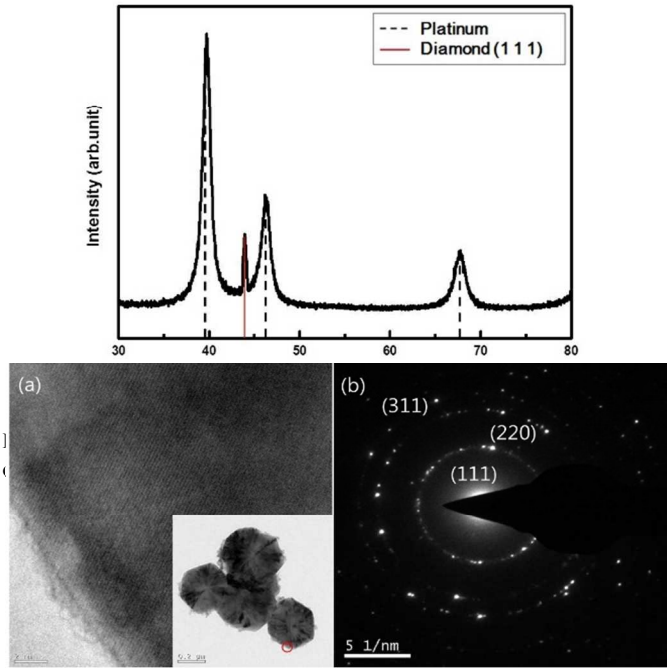

Fig. 3. (a) and inset in (a) TEM images of the BDD support material fabricated by ESA/CVD and (b) corresponding SAED pattern of the diamond (1 1 1) plane.

Fig. 3 shows the TEM images of the BDD particles. As shown in Fig. 3(a), the BDD particle size was approximately 200 nm with a uniform size distribution. Therefore, the nanodiamonds were uniformly grown and well distributed by the ESA/HF-CVD method. The measured *d*-value of the lattice fringe was 0.2 nm, which was indexed as the (1 1 1) diamond plane, as seen in the corresponding SAED pattern [Fig. 3(b)]. The SAED ring patterns were measured as the radius from the pattern's center and compared to the known *d*-spacings of diamond. According to the calculated *d*-spacings, this material was identified as diamond, where the ring spots clearly represent the (1 1 1), (2 2 0), and (3 1 1) diamond planes. The TEM images shown in Fig. 4 show that the Pt nanoparticles are

distributed uniformly on the three different support materials, *i.e.*, the carbon powder Vulcan XC-72 [Fig. 4(a)], MWCNTs [Fig. 4(b)], and BDD [Fig. 4(c)]. The average particle size of the electrocatalysts was measured to be 2.3 nm, which satisfies the criteria for commercial electrocatalysts.[31,33]

Electrochemical properties

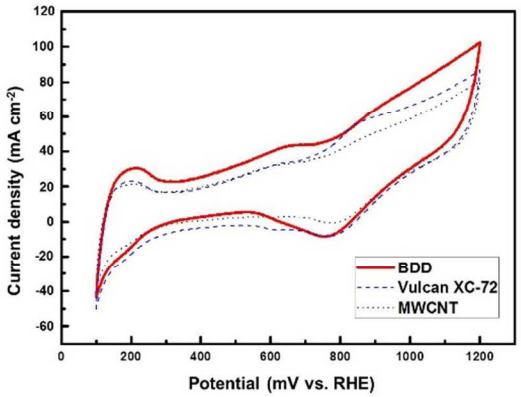

Fig. 5. CV curves of BDD (solid red line), carbon powder Vulcan XC-72 (blue dashed line), and MWCNTs (purple dotted line).

Fig. 5 shows the cyclic voltammograms (CVs) obtained for the three different electrocatalysts prepared by the polyol method. The CV for a Pt support typically consists of two peaks in the forward scan, one at 250 mV (*vs*. RHE), representing the hydrogen (H) desorption/oxidation, and the other at 900 mV, representing the Pt oxidation (PtO_x). Also, two additional peaks appear in the reverse scan, one at 700 mV representing the PtO_x reduction and the other at 200 mV representing the H adsorption/readsorption. As compared to the CV of the Vulcan XC-72, the BDD CV looks similar but it exhibits a higher peak area. The peak area, especially for the H desorption peak, is known to provide a quantitative measurement of the electrochemically available surface area for the catalyst particles. As demonstrated in Fig. 5, the BDD support had the largest surface area of the three materials. However, the size of the Vulcan XC-72 particles (50 nm) is smaller than that of the BDD particles (200 nm), indicating that the BDD support is less agglomerated than the other support materials owing to the individual BDD particles being produced through ESA, as shown in Fig. 1. Therefore, the performance of the BDD support is expected to be better than that of the other support materials.

The unit cell tests of the three different electrocatalysts are shown in Fig. 6, with the polarization curves obtained at 80 °C using H_2/O_2. The voltage and power density of the BDD support is higher than those of the other electrocatalysts as the current density increases. Therefore, the cell performance was clearly enhanced when the BDD support was used except in the low-current-density region. Since a low voltage infers large ohmic losses, the higher voltage of the BDD support in the high-current-density region indicates that the BDD support fabricated by ESA has high electroconductivity and low contact resistance. Owing to differences of electrical conductivity in the polarization direction and perpendicular direction, the MWCNT support showed lower performance than the Vulcan XC-72 and BDD supports. Therefore, BDD is a more suitable support material in terms of performance improvement than the other support materials.

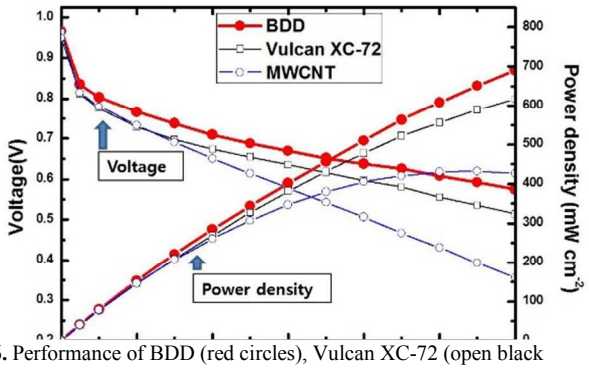

Fig. 6. Performance of BDD (red circles), Vulcan XC-72 (open black squares), and MWCNT (open blue diamonds) electrocatalysts as unit cells. The fuel cell operation conditions were: T_{cell}: 80 °C, anode: H_2, cathode: O_2

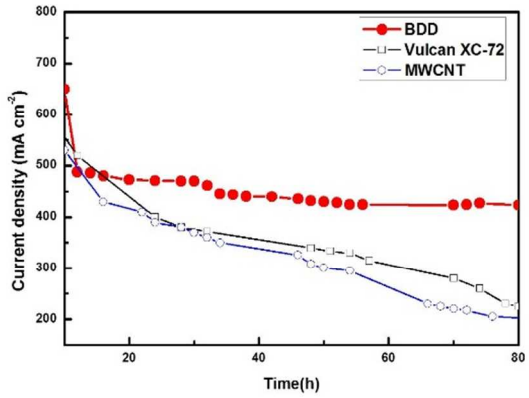

Fig. 7. Accelerated long-term stability test used to compare the durability of the BDD (red circles), carbon powder Vulcan XC-72 (open black squares), and MWCNT (open blue circles) electrocatalysts. The fuel cell operation conditions were: T_{cell}: 90 °C, anode: H_2, cathode: O_2, voltage: 0.6V.

Accelerated long-term stability tests

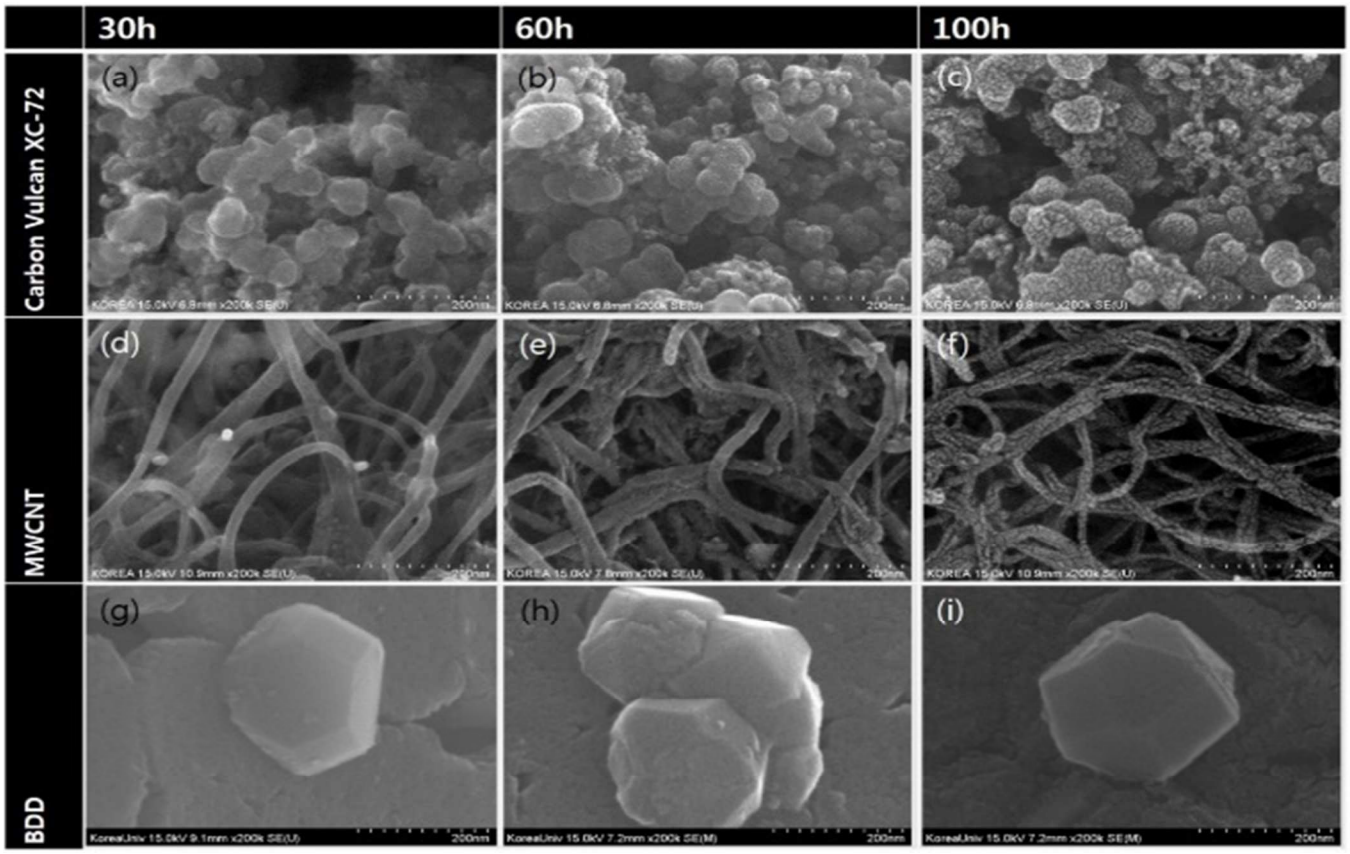

Fig. 8. SEM images showing the surface damage evolution at different points during the 100 h of operation for the carbon powder Vulcan XC-72 at (a) 30 h, (b) 60 h, and (c) 100 h; the MWCNTs at (d) 30 h, (e) 60 h, and (f) 100 h; and the BDD at (g) 30 h, (h) 60 h, and (i) 100 h.

Accelerated long-term stability tests of the different support materials were performed for 100 h of cell operation, including a 10 h activation period. Fig. 7 shows the stability test after the 10-h activation period because the cell performance of the three different catalysts was similar. Each support material, *i.e.*, the Pt/Vulcan XC-72, Pt/MWCNT, and Pt/BDD, was coated on a cathode. During the long-term stability tests, the voltage was maintained at 0.6 V and the unit cells were supplied with a 75 $cm^3 \cdot min^{-1}$ flow rate of hydrogen and air. As shown in Fig. 7, the BDD-supported catalyst had a stabilized current density after 30 h of cell operation, whereas the current densities for the Vulcan XC-72- and MWCNT-supported catalysts steadily decreased up to 80 h. Therefore, the time required to stabilize the BDD-supported catalyst was over 50 h, which was less than that required for the other catalysts. The degradation ratio of the BDD-supported catalyst decreased after 10 h and stabilized after 30 h. In comparison, the degradation tendencies of the MWCNT- and Vulcan XC-72-supported catalysts did not change after 70 h and were expected to stabilize after 80 h. These results indicate that the durability is dependent on the support material and that the BDD support enhanced the durability and stability of the electrode as compared to the commercial Vulcan XC-72 support.

Durability test analyses

Fig. 8 shows the SEM images of the three different catalysts with respect to the operating time of the long-term stability test. Partial surface damage is observed for both the MWCNT and Vulcan XC-72 support materials, and full surface destruction of both supports can be observed after the 100 h long-term stability test. Therefore, decreased

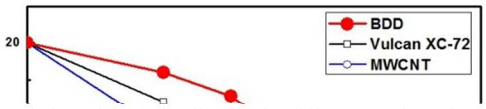

Fig. 9. Degradation of the Pt loading on the different catalysts from the initial state (0 h) to 100 h of operation for the BDD (red circles), carbon powder Vulcan XC-72 (open black squares), and MWCNT (open blue triangles) supports.

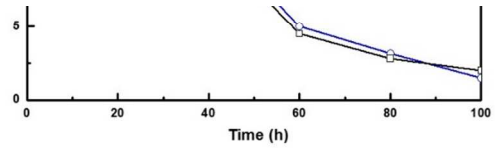

electroconductivity with Pt particle detachment from the support surface is expected. However, the surface of the BDD support after 100 h of operation is less damaged than that of the MWCNT and Vulcan XC-72 supports after 30 h. Therefore, it

is expected that the BDD support would prevent a decrease in cell performance and Pt particle detachment from the support surface. Fig. 9 shows the component analysis measured by energy dispersive X-ray (EDX). The amount of Pt on the MWCNT and Vulcan XC-72 catalysts was reduced by 60% and 70%, respectively, after 100 h of operation as compared to their initial states. In contrast, the amount of Pt on the BDD support was reduced by only 30% after 100 h of operation. This evidence supports the above theory, *i.e.*, Pt detachment from the MWCNT and Vulcan XC-72 catalysts is more severe than that from the BDD catalyst.

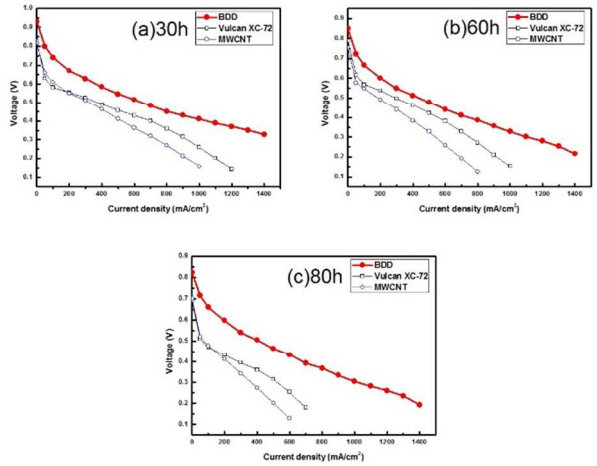

Fig. 10 shows the polarization curves of the unit cells with respect to the operation time. The degradation ratio of the unit cell performance increased with increasing operation time, following a tendency similar to that of the support damage shown in Fig. 8. Despite the small difference in performance between the BDD support and the other supports at 30 h (20% and 25%, respectively), the difference increased to 45% and 80%, respectively, after 80 h of operation. The slopes of the polarization curves decline steeply at 80 h of operation for both the MWCNT and Vulcan XC-72 supports, and this demonstrates that the Pt particles detached from the support material. The performance of the unit cells after 100 h for both the MWCNT and Vulcan XC-72 supports is meaningless because the amount of remaining Pt is negligible, as shown in Fig. 9. On the other hand, the slope of the BDD support's polarization curve decreases at a slower rate, with less performance degradation than was seen with the MWCNT and Vulcan XC-72 supports. Accordingly, the BDD-supported catalyst performed better than the other catalysts, improving the electrode's durability.

Fig. 10. Polarization curves of BDD (red circles), carbon powder Vulcan XC-72 (open black squares), and MWCNT (open blue triangles) supports for (a) 30 h, (b) 60 h, and (c) 80.

Conclusions

In this study, a BDD material was investigated as an electrocatalyst support in PEMFCs. The BDD support was fabricated by the ESA/HF-CVD method. From the XRD data and SEM and TEM images, the generation of diamond crystals was confirmed, and the BDD support particle sizes were approximately 150 nm. According to the CV test results, the surface area was larger than that of the other catalysts, even though the BDD particle size was larger than that of the MWCNT and Vulcan XC-72 support materials. The unit cell tests and the accelerated long-term stability tests revealed that the BDD material performed better than the MWCNT and Vulcan XC-72 supports, thus enhancing the electrode durability in PEMFCs. The MWCNT and Vulcan XC-72 supports showed degraded surfaces under PEMFC operating conditions. However, the surface of the BDD support did not change from its initial state under the accelerated stability test. Owing to the improved stability of the BDD support, Pt detachment under PEMFC operation was reduced, and the durability and stability of the BDD-supported electrode was enhanced. Thus, the BDD material proved to be a more durable electrode support than other conventional carbon support materials.

Notes and references

Department of Materials Science and Engineering, Korea University, 5-1 Anam-Dong, Sungbuk-Ku, Seoul 136-701, South Korea
*Corresponding author: Phone: 82-2-3290-3212,
Fax: 82-2-928-3584, and Email: dslim@korea.ac.kr

[1] J. Wee, K. Lee, S. Kim, *J. Power Sources*, 2007, **165**, 667-677.
[2] H. Liu, C. Song, L. Zhang, J. Zhang, H. Wang, D. Wilkinson, *J. Power*
Sources, 2006, **155**, 95.
[3] P. Costamagna, S. Srinivasan, *J. Power Sources*, 2001, **102**, 242.
[4] K. Sopian, W.R. Wan Daud, *Renew. Energy*, 2006, **31**, 719.
[5] J. Divisek, H. F. Oetjen, V. Peinecke, V. M. Schmidt, U. Stimming, *Electrochem. Acta*, 1998, **43**, 3811-3815.
[6] J. J. Baschuk, X. Li, Int. *J. Energy Res*., 2001, **25**, 695-713.
[7] J. Xie, D. Wood, D. Wayne, T. Zawodzinski, P. Atanassov, R. Borup, *J. Electrochem. Soc*., 2005, **152**, A104.
[8] M. Mathias, H. Gasteiger, R. Makharia, S. Kocha, T. Fuller, J. Pisco, *Abstr. Pap. Am. Chem. Soc*., 2004, **228**, U653.
[9] S.D. Knights, K.M. Colbow, J. St-Pierre, D.P. Wilkinson, *J. Power Sources*, 2004, **127**, 127.
[10] D.A. Stevens, J.R. Dahn, *Carbon*, 2005, **43**, 179.
[11] Y-B. Lee, C-H. Lee, K-M. Kim, D-S. Lim, *Int. J. Hydrogen Energ*., 2011, **36**, 7621-7627.
[12] K. Kang, S. Park, H. Ju, *Solid State Ionics*, 2014, **262**, 332-336.
[13] J.W. Lim, D.G. Lee, *Int. J. Hydrogen Energ*., 2013, **95**, 557-563.
[14] S. Ohyagi, T. Sasaki, *Electrochim. Acta*, 2013, **102**, 336.
[15] Y. Li, F. Quan, L. Chen, W. Zhang, H. Yu and C. Chen, RSC Adv., 2014, **4**, 1895-1899
[16] F. Saeed, M. Saidan, A. Said, M. Mustafa, A. Abdelhadi, S. Al-Weissi, *Energ. Convers. Manag*., 2013, **75**, 36.
[17] S. Shan, J. Luo, J. Wu, N. Kang, W. Zhao, H. Cronk, Y. Zhao, P. Joseph, V. Petkov and C. Zhong, RSC Adv., 2014, **4**, 42654-42669.

[18] D. Ham, C. Pak, G. Bae, S. Han, K. Kwon, S. Jin, H. Chang, S. Choi and J. Lee, Chem. Commun., 2011,**47**, 5792-5794.
[19] G.S. Tasic, S.S. Miljanic, M.P.M. Kaninski, D.P. Saponjic, V.M. Nikolic, *Electrochem. Commun*., 2009, **11**, 2097.
[20] W.E. Mustain, K. Kepler, J. Prakash, *Electrochem. Commun*., 2006, **8**, 406-410.
[21] J. Xi, J. Wang, L. Yu, X. Qiu and L. Chen, Chem. Commun., 2007, 1656-1658
[22] P. Yu, M. Pemberton, P. Plasse, *J. Power Sources*, 2005, **144**, 11-20.
[23] H.A. Gasteiger, S.S. Kocha, B. Sompalli, F.T. Wagner, *Appl. Catal. B*, 2005, **46**, 9.
[24] L. Protsailo, A. Haug, *208th Meeting of the ECS*, Los Angeles, 2005, Abstract 1023.
[25] J. Zhang, S. Tang, L. Liao, W. Yu, J. Li, F. Seland, G.M. Haarberg, *J. Power Sources*, 2014, **267**, 706-713.
[26] A. Zana, C. Rüdiger, J. Kunze-Liebhäuser, G. Granozzi, N.E.A. Reeler, T. Vosch, J.J.K. Kirkensgaard, M. Arenz, *Electrochim. Acta*, 2014, **139**, 21-28.
[27] G. R. Salazar-Banda, K. I.B. Eguiluz, L. A. Avaca, *Electrochem. Commun*., 2007, **9**, 59-64.
[28] L. Guo, V. M. Swope, B. Merzougui, L. Protsailo, M. Shao, Q. Yuan, G. M. Swain, *J. Electrochem. Soc*., 2010 **157**, A19-A25.
[29] J.H. Kim, S.K. Lee, O.M. Kwon, D.S. Lim, *J. Nanosci. Nanotechnol*., 2009, **9**, 4121-4127.
[30] D. Lee, S. Hwang, I. Lee**,** *J. Power Sources*, 2006, **160**, 155-160.
[31] K. Wikander, H. Ekström, A.E.C. Palmqvist, G. Lindbergh, *Electrochem. Acta*, 2007, **52**, 6848.
[32] M.C. Denis, M. Lefevre, D. Guay, J.P. Dodelet, *Electrochem. Acta*, 2008, **53**, 5142.